Alexandria Engineering Journal (2012) 51, 263–268

Alexandria University

Alexandria Engineering Journal

www.elsevier.com/locate/aej
www.sciencedirect.com

ORIGINAL ARTICLE

Fuzzy logic based controller for five-phase induction motor drive system

Z.M.S. El-Barbary

Department of Electrical Engineering, KFS University, Egypt
Department of Electrical Engineering, KK University, Saudi Arabia

Received 7 June 2012; revised 7 October 2012; accepted 9 October 2012
Available online 6 November 2012

KEYWORDS

Five phase induction motor;
Five phase inverter;
Fuzzy logic;
Digital Signal Processor (DSP)

Abstract This paper presents fuzzy logic based controller for five-phase induction motor drives. The controller is based on indirect rotor field oriented control technique. The complete control scheme including the fuzzy logic is experimentally implemented using a digital signal processing board for a laboratory five-phase induction motor, Simulation is carried out by using the Matlab/Simulink package. The performance of the proposed system is investigated at different operating conditions. The proposed controller is a suitable to high performance five-phase induction motor drives. Simulation and experimental results validate the proposed approaches.

1. Introduction

In the last few decades, induction motor (IM) has been recognized as a workhorse in the industry because its reliable efficiency and easy build and high robustness. Multi-phase machines have wide of applications in aerospace, transportation and textile industry. Three-phase drives are widely used in electrical drive applications. However, multi-phase drives have many advantages over conventional three-phase drives such as: reducing the current per phase without increasing the voltage per phase, reducing the rotor harmonic currents, reducing the amplitude and increasing the frequency of torque pulsations, and lowering the dc-link current harmonics and higher reliability.

Many researches [1–5] stated that increasing the number of phases leads to an increase the torque per rms ampere for the same machine volume.

Multi-phase system is required for high power applications to reduce stress on the switching devices. There are two approaches for supplying high power systems; the first one is the use of multilevel inverters supplying three-phase machines and the second one is multi leg inverters supplying multiphase machines.

It is worthy to mention that there is a similarity in switching schemes between the two approaches: The additional switching devices increase the number of voltage levels in multilevel inverter while in multi-leg inverter, the additional number of switching devices increases the number of phases [6].

The recent research works on multiphase machines can be categorized into multi-phase pulse width modulation (PWM) techniques for multiphase machines, harmonic injection to

E-mail address: z_elbarbary@yahoo.com

Peer review under responsibility of Faculty of Engineering, Alexandria University.

Production and hosting by Elsevier

1110-0168 © 2012 Faculty of Engineering, Alexandria University. Production and hosting by Elsevier B.V. All rights reserved.
http://dx.doi.org/10.1016/j.aej.2012.10.005

produce more torque and to achieve better stability, fault tolerant issues of multi-phase motor drives, series/parallel connected multi-phase machines [6]. In Refs. [7,8], described an n-phase space vector pulse width modulation (SVPWM) in terms of applied times available switching vectors on the basis of the space vector concept. Many studies have been made on control met hoods and running performance of five phase drive with two level inverter. However other researches [9] have studies the multi-phase two level nonsinusoidal SVPWM.

The power rating of the converter should meet the required level for the machine and driven load. However, the converter ratings cannot be increased over a certain range due to the limitation of the power rating of semiconductor devices. One solution to this problem is using multi-level inverter, where switches of reduced rating are employed to develop high power level converters. The advent of inverter fed-motor drives also removed the limits of the number of motor phases. This fact allows designing machines with more than three phases and emphasizes investigation and applications of multi-phase motor drives [10].

The five-phase induction motor drives have more space voltage vectors than the three-phase induction motor drives. The increased number of vectors allows the generation of more elaborate switching vector table, in which the selection of the voltage vectors is made based on the real-time values of the stator flux and torque variations.

The aim of this paper is to design and implement a speed control scheme of 5-phase induction motor drive system using fuzzy logic controller (FLC). In which, the system control parameters are adjusted by a fuzzy rule based system, which is a logical model of the human behavior for process control. The main advantages of FLC over the conventional controllers are that the design of FLC does not need the exact mathematical model of the system, and it can handle nonlinear functions of arbitrary complexity.

The speed control algorithm is based on the indirect vector control. A specific FLC for 5-phase induction motor drive has been designed and successfully implemented in real time. The performance of the proposed fuzzy speed controller is investigated theoretically and experimentally at different dynamic operating conditions.

2. Mathematical model of five-phase induction motor

Squirrel-cage five-phase induction motor is represented in its d–q synchronous reference frame. The winding axes of five-stator winding are displaced by 72°. By increasing the number of phases, it is also possible to increase the torque per ampere for the same machine volume. In this analysis the iron saturation is neglected. The general equations of the five-phase induction motor can be introduced as follows:

The stator quadrature-axis voltage is given by:

$$V_{qs} = R_s i_{qs} + \frac{d\lambda_{qs}}{dt} + \omega\lambda_{ds} \quad (1)$$

The stator direct-axis voltage is given by:

$$V_{ds} = R_s i_{ds} + \frac{d\lambda_{ds}}{dt} + \omega\lambda_{qs} \quad (2)$$

For the stationary reference frame $\omega = 0$, substitute into Eqs. (1) and (2) yields:

$$V_{qs} = R_s i_{qs} + \frac{d\lambda_{qs}}{dt} \quad (3)$$

$$V_{ds} = R_s i_{ds} + \frac{d\lambda_{ds}}{dt} \quad (4)$$

The stator q-axis flux linkage is given by:

$$\lambda_{qs} = L_s i_{qs} + L_m i_{qr} = (L_{ls} + L_m) i_{qs} + L_m i_{qr} \quad (5)$$

$$\lambda_{qs} = L_{ls} i_{qs} + L_m (i_{qr} + i_{qs}) \quad (6)$$

The stator d-axis flux linkage is given by:

$$\lambda_{ds} = L_s i_{ds} + L_m i_{dr} = (L_{ls} + L_m) i_{ds} + L_m i_{dr} \quad (7)$$

$$\lambda_{ds} = L_{ls} i_{ds} + L_m (i_{dr} + i_{ds}) \quad (8)$$

The electromagnetic torque is given by:

$$T_e = \frac{5}{2}\frac{p}{2}(\lambda_{ds} i_{qs} - \lambda_{qs} i_{ds}) \quad (9)$$

$$T_e - T_l = j\frac{d\omega}{dt} + B\omega \quad (10)$$

where I_{qs} is the stator q-axis current, I_{ds} the stator d-axis current, I_{qr} the rotor q-axis current, I_{dr} the rotor d-axis current, L_s the stator equivalent inductance, L_{ls} the stator leakage inductance, L_m the magnetizing inductance, T_l the load torque, J the inertia of motor and B the friction coefficient.

3. Control scheme and design of FLC for five-phase IM

3.1. Control scheme

The schematic diagram of the FLC-based indirect field oriented control is shown in Fig. 1. The basic configuration

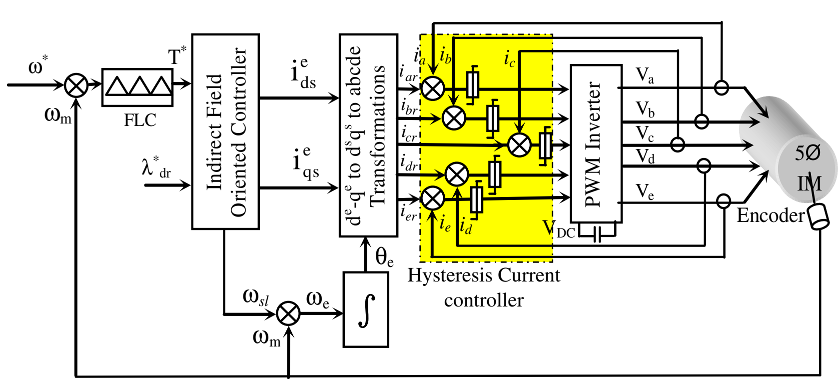

Figure 1 Block diagram of the proposed speed control system.

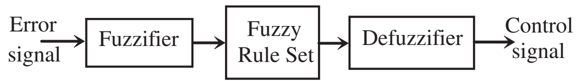

Figure 2 Fuzzy controller.

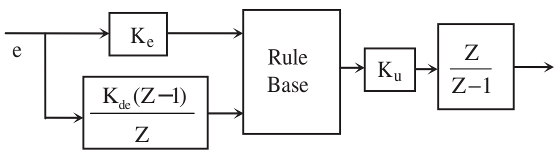

Figure 3 Fuzzy logic PI controller.

Table 1 Fuzzy rule.

Error					
ERROR RATE OF CHANGE	NM	NB	ZE	PB	PM
NM	NM	NM	NM	NP	ZE
NB	NM	NM	NB	ZE	PB
ZE	NM	NB	ZE	PB	PM
PB	NB	ZE	PB	PM	PM
PM	ZE	PB	PM	PM	PM

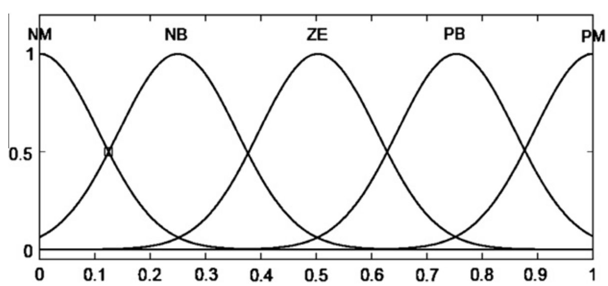

Figure 4 Error memberships.

of the drive consists of an IM fed by a current controlled 5-phase voltage source inverter. The block diagram of the fuzzy logic controller in this work is marked in Fig. 1. In this FLC, the present sample of the speed error, and the present sample of the change of speed error, are the inputs while the present q-axis command current $i^*_q(n)$ is the output. The currents $i^*_q(n)$ and $i^*_d(n)$ are then transformed to a, b, c, d and e current commands using inverse park transform, the phase current commands $i^*_a, i^*_b, i^*_c, i^*_e$ and i^*_d are then compared with the actual currents i_a, i_b, i_c, i_e and i_d to generate the PWM signals, which will fire the power semiconductor devices to produce the actual voltages for the motor.

3.2. Fuzzy logic PI controller

Traditional control systems are usually based on a definite mathematical model often represented by a set of differential equations which describe the relation between input and output variables as well as the system parameters. In contrast, fuzzy logic controller does not require such precise mathematical model [11]. A fuzzy logic controller consists typically of three

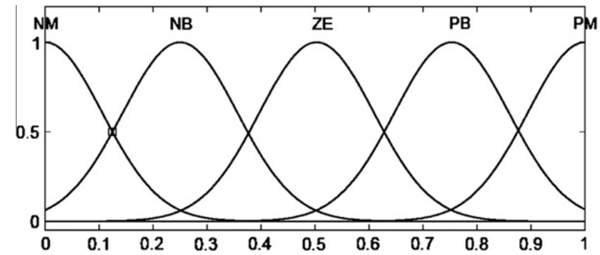

Figure 5 Rate of change of error.

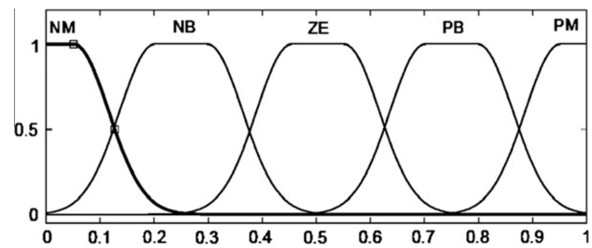

Figure 6 Output membership.

stages or blocks namely, input block, processing block, and output block as illustrated by Fig. 2. The input block converts input signals into appropriate way to pertinence functions. The processing block invokes appropriate rules, generates a result for each rule, and combines the results of those rules. Finally, the output block transforms the combined result into a control signal.

The proposed fuzzy logic PI controller is illustrated in Fig. 3, in which KP = Ku R(Kde) and KI = Ku R(Ke) are the controller proportional and integral gains. The functions R(Kde) and R(Ke) are defined by the controller rule base which is summarized in Table 1. Initially the fuzzy input vector should be defined. It consists of two variables; the speed error $e(t) = \omega_r^* - \omega_r$ and its derivative $\frac{d}{dt}e(t) = \frac{d}{dt}(\omega_r^* - \omega_r)$.

A fuzzy set for input and output variables is designed. Figs. 5 and 6 show the five linguistic variables used for each fuzzy input variable, while the output variable fuzzy set is shown in Fig. 6. The linguistic variables (LV's) used for inputs shown in Figs. 4 and 5 are PM (Positive Medium); PB (Positive Big); ZE (Zero); NB (Negative Big); and NM (Negative Medium). The same LV's are used for the output fuzzy set shown in Fig. 6. A look-up table is required to develop the set of rules, in which the relation between the input variables, $e(t)$ and $\frac{de(t)}{dt}$ are defined and the output variable of fuzzy logic controller can be obtained. The look-up table used in the simulation program is given in Table 1. The output depends on the fuzzy rule expressed as follows;

If(Input1 AND Input2) THEN Output

The torque producing current component is calculated from:

$$I^*_{qs} = \frac{1}{k_t}\frac{(\omega_r^* - \omega_r)}{\lambda^*_{dr}}\frac{K_{ps}[1+\tau_{cs}S]}{\tau_{cs}S} \quad (11)$$

$$I^{e^*}_{ds} = \frac{1}{L_m}\left(1+\tau_r^* p\right)\lambda^{e^*}_{dr} \quad (12)$$

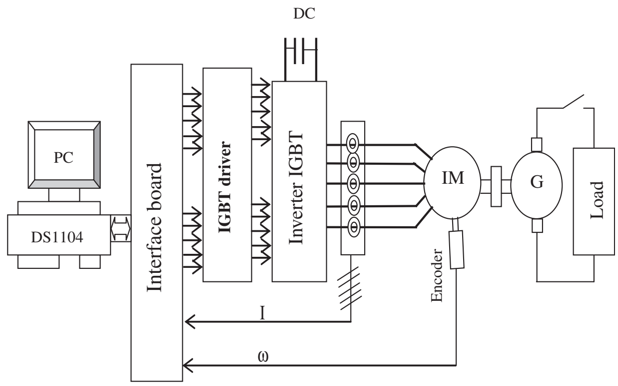

Figure 7 Experimental set-up for DSP-based control of induction motor.

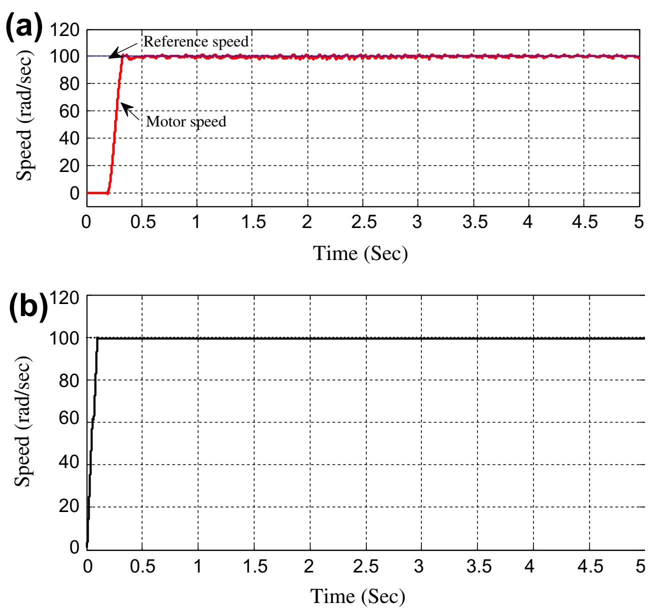

Figure 8 Start-up and steady-state, motor speed. (a) Experimental (b) simulation.

The angular slip frequency command (ω_{sl}^{*}) is:

$$\omega_{sl}^{*} = \frac{L_m}{\tau_r^{*}} \cdot \frac{I_{qs}^{*}}{\lambda_{dr}^{*}} \tag{13}$$

Angular frequency is obtained as follows,

$$\omega_e^{*} = \omega_{sl}^{*} + \omega_r \tag{14}$$

$$\theta_e^{*} = \int \omega_e^{*} \cdot dt \tag{15}$$

$$T_e = K_t |\lambda_{dr}^{e}| I_{qs}^{e} \tag{16}$$

where ω_r is the motor speed, ω_r^{*} the speed reference, K_{ps} the proportional gain PI controller, τ_{cs} the time constant of PI controller, K_t the torque constant $p = \frac{d}{dt}$, ω_{sl}^{*} the angular slip frequency, ω_e^{*} is the angular frequency.

Eq. (16) is similar to that of the separately excited dc motor and denotes that the torque can initially proportional to the q-axis component of the stator current I_{qs}^{*e}, if the q^e-axis component of the flux becomes zero (d^e-axis is aligned with the rotor flux axis), and the d^e-axis component λ_{dr}^{*e} is kept constant. This is the philosophy of the vector control technique. The transformations used for the present system are expressed as follows;

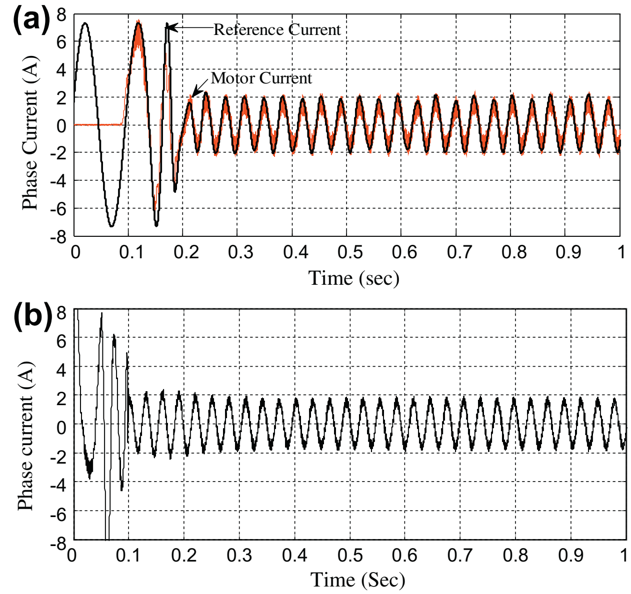

Figure 9 Start-up and steady-state, motor phase-a current. (a) Experimental (b) simulation.

$$q^e - d^e \rightarrow q^s - d^s \begin{Bmatrix} i_{qs}^{s*} = i_{qs}^{e*} \cos\theta_s + i_{ds}^{e*} \sin\theta_s \\ i_{ds}^{s*} = -i_{qs}^{e*} \sin\theta_s + i_{ds}^{e*} \cos\theta_s \end{Bmatrix} \tag{17}$$

where θ_s represents the sum of the slip and rotor angles.

$$qd/abced \begin{Bmatrix} i_{as}^{s*} = i_{qs}^{s*} cos(\theta) + i_{ds}^{s*} \sin(\theta) \\ i_{bs}^{s*} = i_{qs}^{s*} \cos\left(\theta - \frac{2\pi}{5}\right) + i_{ds}^{s*} \sin\left(\theta - \frac{2\pi}{5}\right) \\ i_{cs}^{s*} = i_{qs}^{s*} \cos\left(\theta - \frac{4\pi}{5}\right) + i_{ds}^{s*} \sin\left(\theta - \frac{4\pi}{5}\right) \\ i_{ds}^{s*} = i_{qs}^{s*} \cos\left(\theta + \frac{4\pi}{5}\right) + i_{ds}^{s*} \sin\left(\theta + \frac{4\pi}{5}\right) \\ i_{es}^{s*} = i_{qs}^{s*} \cos\left(\theta + \frac{2\pi}{5}\right) + i_{ds}^{s*} \sin\left(\theta + \frac{2\pi}{5}\right) \end{Bmatrix} \tag{18}$$

3.3. Five phase inverter

The modulated phases voltages of five phase inverter fed five phase induction motor are introduced as a function of switching logic NA, NB, NC, ND and NE of power switches by the following relations:

$$\begin{bmatrix} V_{as} \\ V_{bs} \\ V_{cs} \\ V_{ds} \\ V_{es} \end{bmatrix} = \frac{V_{dc}}{5} \begin{bmatrix} 4 & -1 & -1 & -1 & -1 \\ -1 & 4 & -1 & -1 & -1 \\ -1 & -1 & 4 & -1 & -1 \\ -1 & -1 & -1 & 4 & -1 \\ -1 & -1 & -1 & -1 & 4 \end{bmatrix} \begin{bmatrix} NA \\ NB \\ NC \\ NE \\ ND \end{bmatrix} \tag{19}$$

The per-phase switching state having a range of N = 0, 1.

4. Results and discussion

To verify the validity of the proposed system, an induction motor vector control system was constructed. Fig. 7 shows a block diagram of the experimental system, which was com-

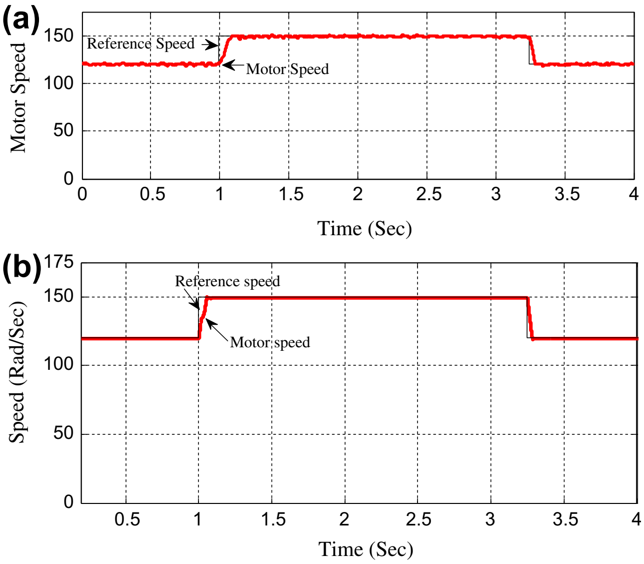

Figure 10 Speed step up and step down changes, motor speed. (a) Experimental (b) simulation.

posed of a DSP board DSP 1104 which is based on 32-bit floating point DSP TI TMS32OC3I. The board is also equipped with a fixed point 16 bit TMS320P14 DSP which is used as a slave processor [12], Five phases currents i_a, i_b, i_c, i_e and i_d are sensed by Hall-effect current transducers. These signals are fed to the DSP through the signal conditioning circuit. Also the speed of the rotor is sensed by 2048 PPR incremental encoder for detecting the motor speed and fed to the encoder interface on the DSP board. The control algorithm is executed by 'Simulink' and downloaded to the board through host computer. The outputs of the board are ten logic signals, which are fed to the, 5-phase inverter through driver isolation circuits. The sampling time for mental implementation is chosen as 100 s. Also, the proposed control system shown in Fig. 1 is designed for a simulation investigation. Simulation is carried out using the general purpose simulation package Matlab/Simulink [13], Simulation and experimental results are presented to show the effectiveness of the proposed scheme at different operating conditions. These results are classified into two categories; the first represents start-up and steady-state while the second represents the dynamic performance.

4.1. Starting and steady state performance

Start-up and steady-state results are illustrated by Figs. 8 and 9. Fig. 8a and b shows the motor speed. Fig. 8a shows the speed signals obtained in real time, whereas Fig. 8b shows the corresponding signals obtained from simulation. There is a good correlation between these signals, from start-up point up to the steady state value. Fig. 9a shows the motor phase current obtained in real time. Whereas, Fig. 9b shows the corresponding signal obtained from simulation. In the two figures, the current signals are of sine wave profiles on which controller switching transients are shown.

4.2. Dynamic performance

For studying the dynamic performances of proposed system, a series of measurements and simulations have been carried out. In this respect, the dynamic response of the proposed algorithm is studied under speed step change.

To study the dynamic response of the control system due to a step changes in the command of speed, the motor is subjected to step changes in the speed command at no load to evaluate its performance. At t = 1 s. The motor speed command is changed from 120 rad/s to 150 rad/s and return back to 120 rad/s after 2.25 s. Fig. 10a and b shows the motor speed

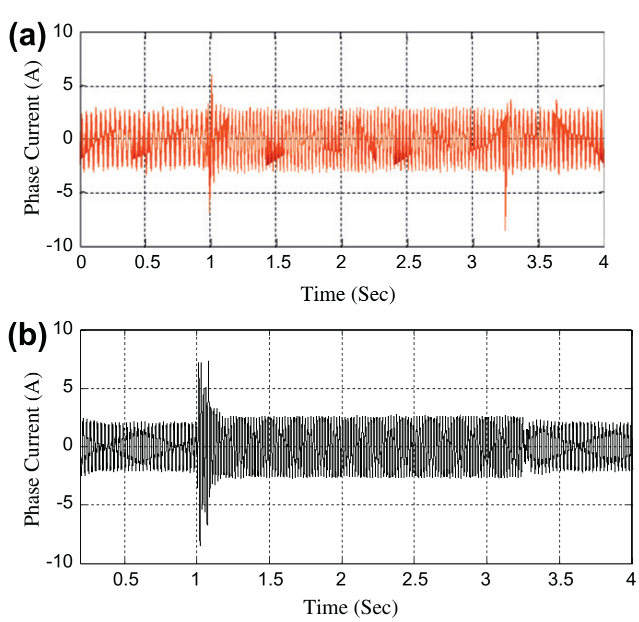

Figure 11 Speed step up and step down changes, motor phase-a current. (a) Experimental (b) simulation.

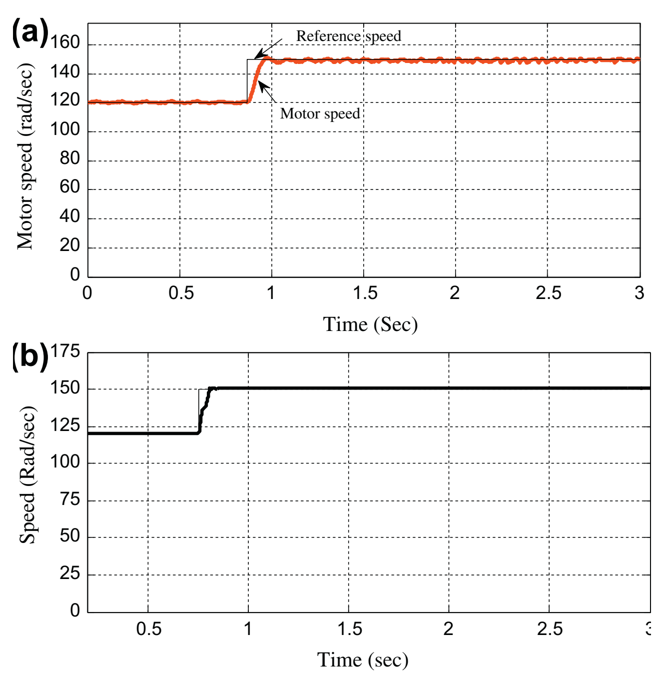

Figure 12 Speed step up change, motor speed. (a) Experimental (b) simulation.

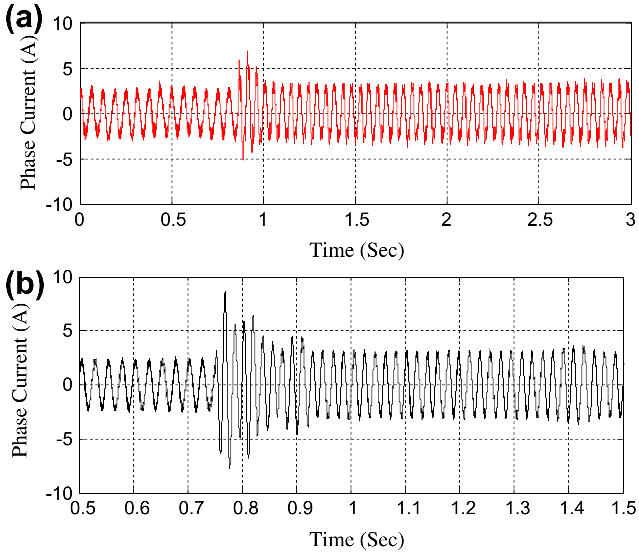

Figure 13 Speed step up change, motor phase-a current. (a) Experimental (b) simulation.

signals corresponding to these step changes. It can be seen that the motor speed is accelerated and decelerated smoothly to follow its reference value with nearly zero steady state error. Fig. 10a shows the speed signal obtained in real time. Fig. 10b shows the corresponding signal obtained from simulation. These results show a good correlation between these speed signals. Phase current corresponding to this speed step changes are shown in Fig. 11a and b respectively. Fig. 11a represents the phase current these results ensure the effectiveness of the proposed controller and shows good behavior of its dynamic response.

To study the response of the control system under load condition, at t = 0.75 s the speed command is changed from 120 rad/s to 150 rad/s at full load. Fig. 12a and b shows the motor speed signals corresponding to these step change. It can be seen that the motor speed is accelerated smoothly to follow its reference value with nearly zero steady state error. These results show a good correlation between these speed signals. Phase current corresponding to this speed step change are shown in Fig. 13a and b respectively.

5. Conclusions

The paper demonstrates the versatile application of fuzzy theory for the control of five-phase induction motor drive system. A simple structure of fuzzy logic controller has been proposed. This structure has been derived from the dynamic model of five-phase induction motor drive system using the vector control technique. The effectiveness of the fuzzy logic controller has been established by performance prediction of an experimental and simulation of five-phase induction motor drive over a wide range operating conditions. The proposed fuzzy logic controller based drive system has been successfully implemented in the real time for the laboratory five-phase induction motor. Simulation and experimental results have confirmed the expected performance of the fuzzy logic controller. The results show that the effectiveness and robustness of the proposed speed control method.

Appendix A

Motor parameter	
No. of poles	4
Stator resistance	7.4826 Ω
Rotor resistance	3.6840 Ω
Rotor leakage inductance	0.0221 H
Stator leakage inductance	0.0221 H
Mutual inductance	0.4114 H
Supply frequency	50 Hz
Motor speed	1500 r.p.m.
Supply voltage	380 volts
Inertia	0.02 kg m^2

References

[1] M. Rizwan Khan, Atif Iqbal, MRAS based sensorless control of a series-connected five-phase two-motor drive system, Journal of Electrical Engineering & Technology 3 (2) (2008) 224–234.
[2] E. Levi, R. Bojoi, F. Profumo, H.A. Toliyat, S. Williamson, Multiphase induction motor drives technology status review. IEE Electric Power Applications 1 (4) (2007) 489–516.
[3] G.K. Singh, Multi-phase induction machine drive research – a survey, Electric Power Systems Research 61 (2002) 139–147.
[4] S. Williamson, A.C. Smith, Pulsating torque and losses in multiphase induction machines, IEEE Transactions on Industry Applications 39 (4) (2003) 986–993.
[5] M. Rizwan Khan, Atif Iqbal, Experimental investigation of five-phase induction motor drive using extended Kalman-filter, Asian Power Electronics Journal 3 (1) (2009) 20.
[6] H. Xu, H.A. Toliyat, L.J. Petersen, Rotor field oriented control of a five-phase induction motor with the combined fundamental and third harmonic currents, in: Proceedings of the IEEE Applied Power Electronics Conference APEC, Anaheim, CA, 2001, pp. 392–398.
[7] H. Xu, H.A. Toliyat, L.J. Petersen, Five-phase induction motor drives with DSP-based control system, IEEE Transactions on Power Electronics 17 (2) (2002) 524–533.
[8] J.W. Kelly, E.G. Strangas, J.M. Miller, Multi-phase space vector pulse width modulation, IEEE Transactions on Energy Conversion 18 (2) (2003) 259–264.
[9] G. Grandi, G. Serra, A. Tani, General analysis of multi-phase systems based on space vector approach, in: Proceedings of the EPEPEMC Conference, Portoroz, Slovenia, 2006, pp. 834–840.
[10] H.A. Toliyat, R. Shi, H. Xu, A DSP-based vector control of five-phase synchronous reluctance motor, in: Proceedings of the IEEE IAS Annual Meeting, Rome, Italy, 2000, CD-ROM Paper No.40_05.
[11] Chen. C-Li, Chang. M-Hui, Optimal design of fuzzy sliding mode control: a comparative study, International Journal on Fuzzy Sets Systems 93 (1998) 37–48.
[12] dSPdCE, Digital signal processing control engineering. Manual Guide. GmhH. Paderhom~Germany, 1996.
[13] Matlab/Simulink Toolbox User's Guide, The Math works Inc., Natick, MA, USA, May 1998.